Chapter 2

A Program for Evaluating Stellar Activity vs. Age

To pursue the goal of characterizing stellar activity by stellar age, an effective observing program must be determined. Once the target objects have been chosen, the number of observations that are needed and what photometric precision will be required must be decided. The photometric precision necessary will dictate the observational strategy.

2.1 Program Objects

Since the goal is to characterize stellar activity for solar-type stars, the first requirement for the program objects is that they be of solar composition. Secondly, the objects must span the age gap between observations of young clusters and the Sun (discussed in Chapter 1). Finally, observational considerations and precision requirements demand that the objects are relatively bright (therefore relatively nearby) and contain enough stars to meet our statistical goals.

The clusters NGC 7789, NGC 6819, M67, and NGC 188 fulfill these requirements. The sections below discuss each cluster briefly, and Table 2.1 summarizes their properties.

2.1.1 NGC 7789

NGC 7789 is the youngest cluster in our program, at an age of 1.6 Gyr (Gim et al. 1998). It lies near the plane of the galaxy ($b = -5.36°$) at a distance of 2.75 kpc (Gim et al. 1998). Estimates of the reddening of the cluster range from $E(B-V) = 0.23$ (Arp 1962) to $E(B-V) = 0.28$ (Gim et al. 1998). Estimates of the cluster's metallicity using the giant branch slope-metallicity relation gives $\left[\frac{Fe}{H}\right] = -0.62$ (Tiede, Martini & Frogel 1997), while near-IR photometry estimates yield $\left[\frac{Fe}{H}\right] = -0.25$ (Vallenari, Carraro & Richichi 2000). An image of NGC 7789 is shown in Figure 2.1.

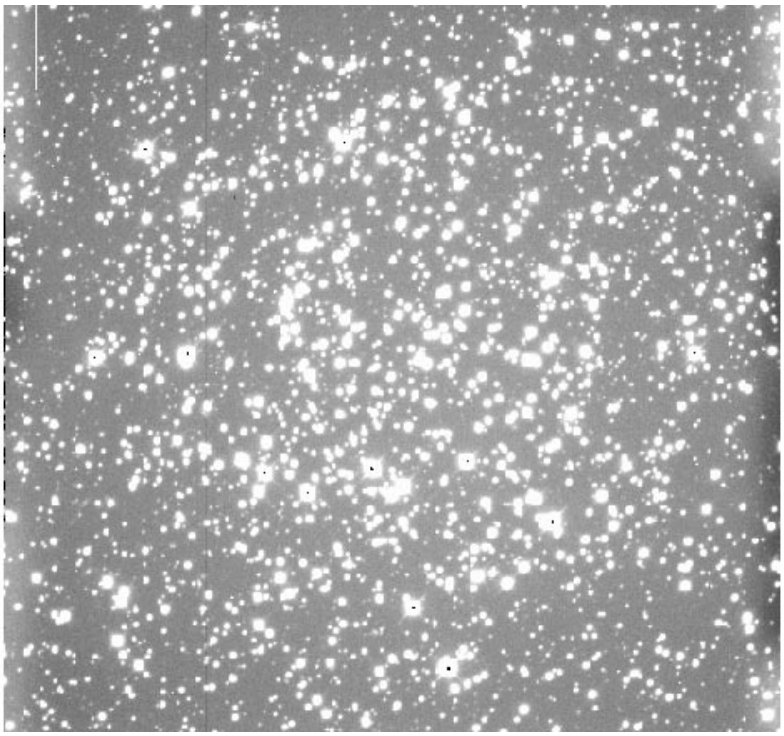

Figure 2.1: This image of NGC 7789 was taken at MLO on UT 1998 Jul 28. The exposure was 120 s through the V filter. The image is $14' \times 14'$; north is up and east is to the right. The image was scaled from 10 to 114 ADUs.

2.1.2 NGC 6819

NGC 6819 is approximately 2.5 Gyr in age (Kalirai et al. 2001). It is located somewhat above the plane of the galaxy ($b = 8.47°$) at a distance of 2.50 kpc (Kalirai et al. 2001). Reddening estimates range from $E(B-V) = 0.1$ (Kalirai et al. 2001) to 0.27 (Janes & Phelps 1994). Using high-dispersion spectra of red clump stars, Bragaglia et al. (2001) have made very good estimates of both the extinction, $E(B-V) = 0.14$ and the metallicity, $\left[\frac{Fe}{H}\right] = 0.09$. Other metallicity estimates have ranged from -0.1 (Friel & Janes 1993) to 0.05 (Thogersen, Friel & Fallon 1993). NGC 6819 is shown in Figure 2.2.

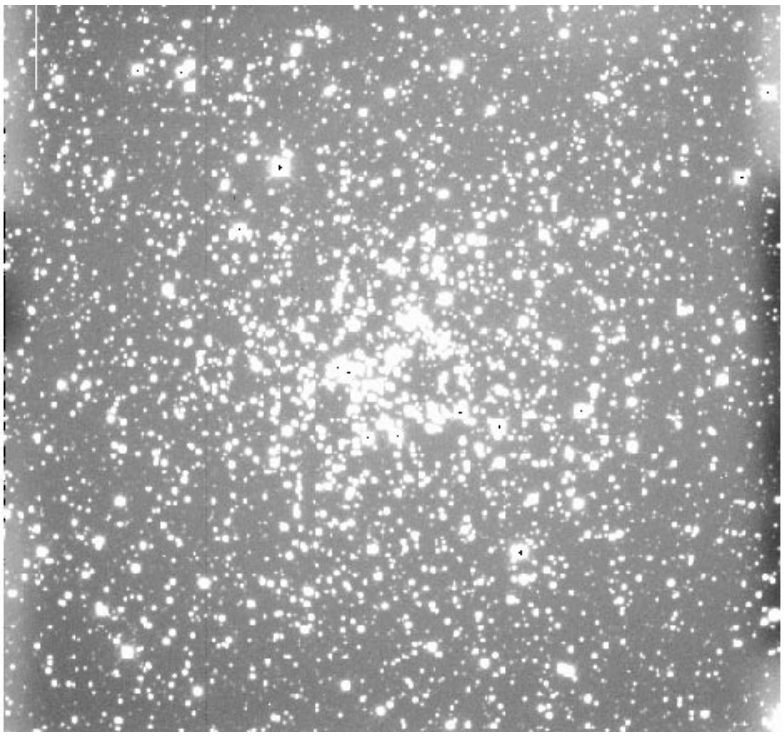

Figure 2.2: This image of NGC 6819 was taken at MLO on UT 1998 Jul 28. The exposure was 180 s through the V filter. The image is $14' \times 14'$; north is up and east is to the right. The image was scaled from 34 to 178 ADUs.

2.1.3 M67

M67 is a nearby cluster (Fan et al. 1996, 0.78 kpc) well above the plane of the galaxy ($b = 31.72°$). Its age is approximately 4.0 Gyr (Dinescue et al. 1995; Fan et al. 1996). Photometry of the cluster by Montgomery, Marschall & Janes (1993) have yielded a reddening of $E(B-V) = 0.05$. High-resolution spectra of helium-burning clump stars have given a metallicity of $\left[\frac{Fe}{H}\right] = -0.03$ (Tautvaisiene et al. 2000), while other metallicity measurements have been as low as -0.10 (Fan et al. 1996). M67 is shown in Figure 2.3.

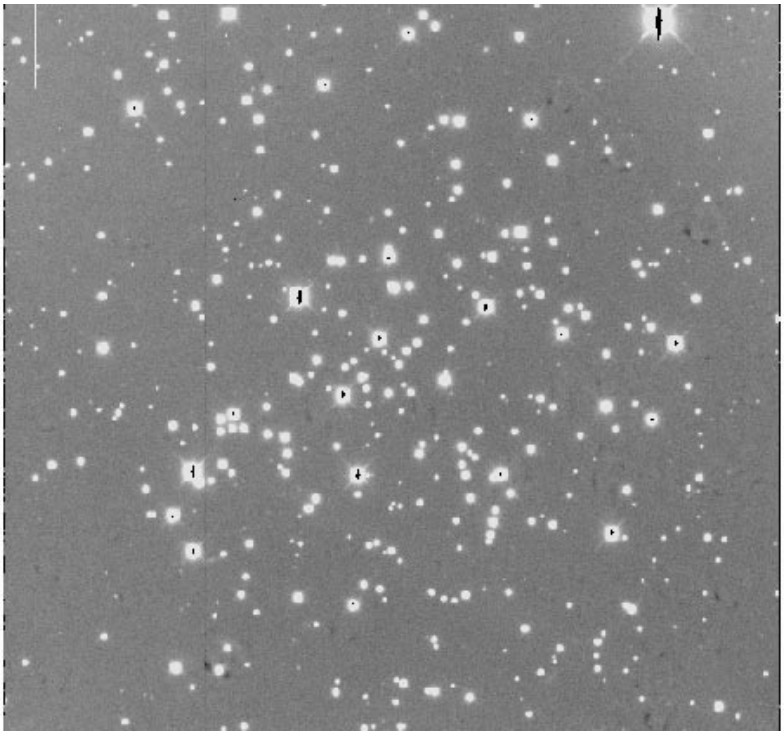

Figure 2.3: This image of M67 was taken at MLO on UT 1998 Oct 14. The exposure was 60 s through the R filter. The image is $14' \times 14'$; north is up and east is to the right. The image was scaled from 324 to 488 ADUs.

2.1.4 NGC 188

NGC 188 is an old cluster (Sarajedini et al. 1999, 7.0 Gyr) that lies near the celestial pole, above the plane of the galaxy ($b = 22.46°$). High-precision UBVRI photometry by

Sarajedini et al. (1999) led to a distance modulus of 11.44 mag and $E(B-V) = 0.09$, assuming solar metallicity. Friel (1995) lists the metallicity as $\left[\frac{Fe}{H}\right] = -0.05$. NGC 188 is shown in Figure 2.4.

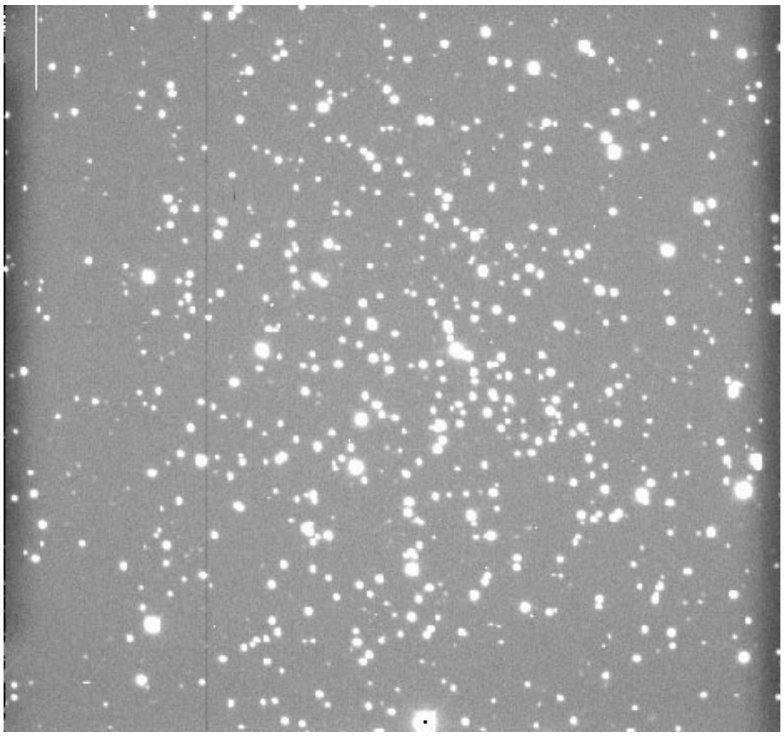

Figure 2.4: This image of NGC 188 was taken at MLO on UT 1998 Jul 29. The exposure was 60 s through the V filter. The image is $14' \times 14'$; north is up and east is to the right. The image was scaled from 2 to 67 ADUs.

2.2 Differential Ensemble Photometry

CCD differential photometry has long been used to take precise relative photometric measurements under sky conditions that would render absolute photometry impossible (Howell & Jacoby 1986, for example). The prevailing assumption is that sky transparency gradient will be negligible over the field of view observed by one image.

In the most basic form of CCD differential photometry, the target star and a comparison star would be imaged in one frame. Using simple aperture photometry, the difference

Cluster	l(°)	b(°)	age (Gyr)	$\left[\frac{Fe}{H}\right]$	E(B-V)	m-M (mag.)
NGC 7789	115.49	-5.36	1.6[1]	−0.25[2]	0.28[1]	12.2[1]
NGC 6819	73.98	8.47	2.5[3]	0.09[4]	0.14[4]	11.99[3]
M67	215.58	31.72	4.0[5,6]	−0.03[7]	0.05[8]	9.46[6]
NGC 188	122.78	22.46	7.0[9]	−0.05[10]	0.09[9]	11.44[9]

Table 2.1: A summary of the properties of the open clusters we will observe. References: 1 - Gim et al. (1998); 2 - Vallenari, Carraro & Richichi (2000); 3 - Kalirai et al. (2001); 4 - Bragaglia et al. (2001); 5 - Dinescue et al. (1995); 6 - Fan et al. (1996); 7 - Tautvaisiene et al. (2000); 8 - Montgomery, Marschall & Janes (1993); 9 - Sarajedini et al. (1999); 10 - Friel (1995).

in magnitude between the target and comparison star can be found. Assuming that the comparison star's brightness does not change, the variability of the target star can be monitored in this way over many CCD frames.

But what if the comparison star is not reliably steady? More comparison stars can be observed as a double check. When observing a rich field, many stars can be used as comparison stars. This set of comparison stars is the *ensemble*; even if some members of the ensemble vary slightly, the average of all the stars should not change much from frame to frame. Thus, each target star may be compared to the ensemble. Target stars may themselves be members of the ensemble for the measurement of the differential magnitude of *another* target star.

In the analysis performed here, a different set of ensemble stars is chosen for each target star. The ensemble stars are chosen to be similar to the target star in brightness, near the target star in the field of view, and similar in color.

2.3 Data Requirements

In planning the observations, the length of the time baseline needed to meet the program goals, how many nights of observations within that baseline, and the precision needed must be determined. I consider here the noise budget for a typical magnitude measurement.

2.3.1 Noise Budget

In order to determine if the photometric errors determined by the computer software are comparable to the expected errors, I have calculated the expected errors following the work of KF92 and also listed the errors computed by the Stellar Photometry Software program (SPS), which is described in § 3.2.

Following KF92, I estimate the relative error for an aperture photometry measurement as the sum of several terms: contributions due to flat fielding uncertainty, to incorrectly centering the photometry aperture, and to counting statistics from both the star and the sky. Assuming that the shape of the stellar profile is Gaussian, the relative error can written as:

$$\delta_{AP}^2 = \frac{2\ln 2}{\pi W^2}\left(\frac{1}{e_{ff}} + \sigma_{ff}^2\right) + \left(\frac{1}{2}\right)^{\left(\frac{2r_{AP}}{W}\right)^2} + \frac{1}{e_{star}} + \frac{\pi r_{AP}^2(e_{sky} + \sigma_{RN}^2)}{e_{star}^2}. \qquad (2.1)$$

The individual quantities and their units are described below.

I used a de-focused V image taken of M67 on UT 2002 Mar 21 as a test case, concentrating on the star in the center of the frame. Since the star's light was spread over more pixels, longer exposure times were possible before saturation. Therefore, the photon noise should be especially low. The integration time of the image was $70s$. The quantities in the equation and values used are as follows:

- W is the FWHM of the star in pixels; from SPS this is 26.96 pix.
- e_{ff} is the number of electrons in one pixel of the flat field used as calibration; from the master V sky flat from the observing run, a sample value is 3.4537×10^4 e^-.
- σ_{ff} is any relative additional flat fielding noise; I assumed this was zero.
- r_{AP} is the aperture photometry radius in pixels, which is set to be 48 pix in SPS.
- e_{sky} is the number of electrons in one pixel due to the sky background; an estimation by *phot* in IRAF showed this to be 2105.83 e^-.

- e_{star} is the number of electrons in the star; again *phot* in IRAF found the sum to be 2.9639×10^7 e^-.

- σ_{RN} is the readout noise of the CCD, which is 17.0 e^-.

Using these values, the relative error is $\delta_{AP} = 0.01235$, which is a magnitude error of 13.33 *mmag*. SPS found an $m_{AP} = 7.1395$ mag and $\sigma_{AP} = 1.6$ mmag for the star described above. However, if the second term, due to offset errors is neglected, the calculation gives a magnitude error of 0.5026 mmag, which is less than that from SPS. (A description of how the errors are calculated by SPS is in § 3.3.1.) This calculation was also done for a star ~ 3.5 mag fainter than this star; the results are listed in Tables 2.2 and 2.3.

A similar calculation can be done for the PSF-fitting photometry errors. From KF92, the equation includes not only flat field, sky, and counting statistics errors, but also the contribution of sky and counting statistics errors to determining the PSF.

$$\delta_{PSF}^2 = \frac{2\ln 2}{\pi W^2}\left(\frac{1}{e_{ff}} + \sigma_{ff}^2\right)\left(\frac{1}{n_{PSF}} + (n+1)\right) + \frac{1}{n_{PSF}e_{PSF}}$$
$$+\pi r_{PSF}^2\left(\frac{e_{sky}+\sigma_{RN}^2}{n_{PSF}e_{PSF}^2}\right) + \frac{n+1}{e_{star}} + \left(\frac{\pi W^2(n+1)^2}{4n\ln 2}\right)\left(\frac{e_{sky}+\sigma_{RN}^2}{e_{star}^2}\right) \qquad (2.2)$$

The new quantities are as follows:

- n_{PSF} is the number of stars used to determine the PSF; in the test case $n_{PSF} = 29$.

- n indicates whether the noise is expected to be dominated by Poisson noise from the star ($n = 1$) or by the sky background ($n = 2$). In this example, $n = 1$.

- e_{PSF} is the average number of electrons in the PSF stars; for this example, this was set to e_{star}, which is slightly high.

- r_{PSF} is the radius of the PSF, which is set to 48 pix in SPS.

This calculations yields $\delta_{PSF} = 0.000381$, or 0.4136 mmag. SPS found the PSF-fitting magnitude for the same star to be 7.1390 with an error of 0.2 mmag. Again, this calculation was repeated for the fainter star, as seen in Tables 2.2 and 2.3.

The aperture magnitude error and PSF magnitude error calculations were repeated for the same two stars, but from an in-focus image. In these cases, $W = 9.62$ pix, $r_{AP} = 18$ pix, and the exposure time was 15 s.

Star Type	Aperture Photometry		
	KF92 mag. error (with pos. offsets, in mmag)	KF92 mag. error (without pos. offsets, in mmag)	SPS mag. error (in mmag)
in-focus, bright	8.5	0.6	1.2
in-focus, faint	8.7	2.3	2.3
de-focused, bright	13.3	0.3	1.6
de-focused, faint	13.5	2.4	1.9

Table 2.2: A summary of the magnitude errors calculated following KF92 versus those from SPS. The first two aperture photometry columns list results when the positional offset error term was included and excluded, respectively (see text).

Star Type	PSF Photometry	
	KF92 mag. error (in mmag)	SPS mag. error (in mmag)
in-focus, bright	0.8	0.5
in-focus, faint	3.1	2.0
de-focused, bright	0.4	0.2
de-focused, faint	2.4	1.0

Table 2.3: A summary of the magnitude errors calculated following KF92 versus those from SPS for PSF photometry.

From examination of Tables 2.2 and 2.3, some conclusions can be drawn. The aperture photometry errors given by SPS fall between the KF92 errors that include the positional offset error and that exclude the offset error term. KF92 determined this error term through simulations using a variety of apertures, so it may not be applicable to our data; however, some contribution is clearly missing from the SPS error calculation. The term seems to more strongly affect the bright star, but that actually is because other noise terms are becoming of equal significance for the faint star.

The PSF errors given by SPS are approximately one-half of those calculated following

the procedure in KF92. This is partially, if not solely, due to the fact that SPS does not include error terms stemming from the Poisson statistics of the stars from which the PSF was constructed.

2.3.2 Time Baseline and Precision

The minimum time baseline needed for the observations will be primarily determined by the rotation period of the stars. According to Soderblom (1983), the youngest stars, in NGC 7789, will rotate in about 12 d, and the oldest stars, in NGC 188, will rotate in about 32 d.

A number of observations will be needed to achieve a reasonable signal-to-noise level. From Scargle (1982), the signal-to-noise of a peak in the power spectrum can be written as:

$$S/N = N_\circ \left(\frac{x_\circ}{2\sigma_\circ} \right)^2, \tag{2.3}$$

where $N_\circ$ is the number of observations, $x_\circ$ is the measurement, and $\sigma_\circ$ is the error in the measurement. The mean of all of the frames taken in one night will be considered one observation, which is $N_\circ$. Using the Sun as an activity guideline, the expected amplitude of variability is $x_\circ \sim 1$ mmag. Table 2.4 shows the minimum number of nights needed to detect this fluctuation with a $S/N = 10$ as a function of magnitude, using typical nightly mean magnitude errors for each magnitude. While it is possible for the minimum number of nights for the stars brighter than V=17 to be observed, it is unlikely that the hundreds of nights of observations necessary for the fainter stars will be acquired. A compromise must be made: either the search will be limited to higher amplitudes of variability, or a lower signal-to-noise will be acceptable.

V (mag)	$\sigma_\circ$ (mmag)	$N_\circ$ (days)
13	0.5	10
14	0.7	20
15	0.7	20
16	1.0	40
17	1.9	144
18	3.9	608

Table 2.4: The number of nights required to detect a 1 mmag variation at each V magnitude, using Equation 2.3.